

DEFORMABLE REGISTRATION OF MALE PELVISES IN CT IMAGES

Yiqiang Zhan^{1,2}, Dinggang Shen^{1,2}, Russell H. Taylor²

1. Sect. of Biomedical Image Analysis, University of Pennsylvania, Philadelphia, PA

2. Center for Computer-Integrated Surgical Systems and Technology, The Johns Hopkins University, Baltimore, MD

ABSTRACT

In this paper, a method for deformable registration of male pelvises in CT images is proposed. It is composed of three major steps. Firstly, an attribute vector is defined for each voxel in the image, and is used to reflect the density distribution of the bone tissues in the neighborhood of that voxel. Different anatomical structures thus own different attribute vectors. Secondly, the match of two images under a particular deformation is evaluated by integrating the similarities of attribute vectors on the corresponding voxels. Finally, a set of hierarchical deformation strategies are employed, in order to avoid the local minimum match of two images. The performance of this deformable registration method has been demonstrated by both synthesized and real CT images of pelvises.

1. INTRODUCTION

Image registration is a process to find an optimal transformation between a pair of images, i.e., the model image and the subject image. It has recently become very active in medical image research with clinical applications, such as diagnosis, longitudinal studies and surgical planning. In our research of constructing a deformable density atlas for bone anatomy [1], image registration also plays a critical role. Only after correctly registering pelvis images, can the corresponding structures across different subjects be found, and thus statistics of bone densities can be collected. In the application of atlas-based pre-surgical planning, the virtual atlas should be robustly registered with the patient's pelvis, in order to apply statistical knowledge to an individual patient. In this paper, we will propose a method for deformable registration of pelvises in CT images.

Many registration methods have been proposed in the literature. Some of them are rigid-body registration methods [2], while others are non-rigid registration methods [3,4,8]. Some of these methods use features such as points, curves or surfaces to guide the matching of two images [4,5], while others use the similarity of intensities to evaluate the matching of two images [6,7]. In our method, an *attribute vector* is employed to evaluate the similarity of two images after deformable registration. An attribute vector is defined for each voxel in the images, and is designed to capture both global and local statistical information of bone tissue distribution in the neighborhood of that voxel. Thus, the similarity of two voxels in the two images can be directly defined as the similarity of their attribute vectors, which

is clearly differs from the intensity similarity measurement used extensively in most registration methods. For increasing the robustness, accuracy, and efficiency of our deformable registration method, the match of attribute vectors in the two images is hierarchically performed.

This paper is organized as follows. Section 2 details our deformable registration method. Section 3 demonstrates the performance of our method by both synthesized and real CT images of pelvises. Section 4 offers conclusions.

2. METHODS

There are two essential problems for image registration, (i) the definition of the image similarity and (ii) the algorithm to find the transformation that maximizes the image similarity, both of which are also the trademarks of different registration methods. In our method, the image similarity is defined as the similarity of attribute vectors that reflect the statistical distribution of bone tissue in the neighborhood. Also, hierarchical deformation strategies are employed, in order to avoid the local minima in image registration. Due to the page limits, we will focus on similarity definition in this paper. For a description of hierarchical deformation strategies, please refer to the HAMMER image registration algorithm [8], since we used the similar deformation strategies as HAMMER's.

2.1. Attribute vectors and their similarity

The definition of the image similarity is a critical problem for image registration. In recent years, a number of similarity measurements have been proposed, such as mean square difference of intensities (MSD) [9], entropy of the difference image (EDI) [10], mutual information (MI) [11] and pattern intensity (PI) [12]. Most of them are based on the image intensity or its statistical distribution. However, for medical image registration, it is important to identify the same anatomical structures across different subjects, in order to improve the accuracy of registration results. Therefore, the similarity measurement should reflect the underlying anatomical similarity rather than the intensity similarity. Shen *et al.* [8] have utilized a concept of "*attribute vector*" for brain MRI image registration. The attribute vector, which is attached to every voxel in the image, includes not only the image intensity and edge information, but also the *geometric moment invariants* (GMI), which is calculated from the spherical neighborhood of each voxel and used to capture the anatomical information around that voxel. By using this definition of attribute vector, two different

anatomical parts of brains that would otherwise appear to be similar can be differentiated.

Built upon the above idea, we also define an attribute vector for each voxel in order to evaluate the similarity between two CT images of pelvises. However, by studying the characters of male pelvises, our attribute vector is designed in a different way compared to that of HAMMER [8]. *First*, our attribute vector is not based on the multi-class tissue classification. In HAMMER, the brain tissues are firstly classified as gray matter, white matter and CSF. Then, most components of the attribute vector, such as edge type and GMI, are produced based on the tissue classification result. Though the pelvis also contains three different tissues, compact bone, spongy bone and marrow, the intensities of these three tissues are not quite differentiated in the CT image and thus easier to misclassify. Moreover, the structure of the pelvis can be simply defined as a dark internal region with an external bright ribbon of similar width. In this way, we can simply classify voxels into two classes, bone or background; and the attribute vector can be computed only for the voxels labeled as bone tissues. *Second*, as the anatomical structure of pelvis is relatively simpler than that of the brain, our attribute vector doesn't include high-order GMIs, which are usually used to represent the complicate geometric features of the object. Actually, our attribute vector captures statistical parameters about the 3-D distribution of the bone tissues around each voxel, the details of which will be described next.

Assume x is a voxel of the image I , its attribute vector $\bar{A}(x, I)$ is composed of four sub-vectors, i.e.

$$\bar{A}(x, I) = [\bar{A}_1(x, I) \ \bar{A}_2(x, I) \ \bar{A}_3(x, I) \ \bar{A}_4(x, I)]. \quad (1)$$

$\bar{A}_1(x, I)$ is a 1x1 vector. It represents the ratio of the bone tissues in x 's neighborhood, which can be presented as

$$\bar{A}_1(x, I) = \frac{\sum_{v \in N(x)} L(v)}{\sum_{v \in N(x)} 1}. \quad (2)$$

Here, $N(x)$ denotes a spherical neighborhood around the voxel x , whose radius is R . $L(v)$ is a membership function that evaluates the degree of voxel v belonging to the bone. In our case, a hard tissue classification method is used, therefore $L(v)$ can be either 1 or 0, corresponding to bone or background, respectively. In future applications, $L(v)$ could also be extended to a fuzzy membership function, whose output can be any real value between 0 and 1.

$\bar{A}_2(x, I)$ is a 1x3 vector. It is the mass center of the bone tissues in x 's neighborhood, and is calculated as follows:

$$\bar{A}_2(x, I) = \left(\sum_{v \in N(x)} L(v) \bullet v / \sum_{v \in N(x)} L(v) - x \right) / R. \quad (3)$$

R is the radius of the spherical neighborhood around the voxel x , and it is used as a normalization factor to guarantee the magnitude of $\bar{A}_2(x, I)$ being no larger than 1.

$\bar{A}_3(x, I)$ and $\bar{A}_4(x, I)$ are 1x3 and 1x1 vectors, respectively. They jointly reflect another important character of bone tissue's distribution, i.e., the largest variation direction of the distribution and its corresponding variation (c.f. Fig. 1). Mathematically, the voxels that locate in x 's neighborhood and belong to the bone can be presented as a set of 3D vectors, $\{v_i | v_i \in N(x) \wedge L(v_i) > t, i = 1 \dots M\}$, where t is a threshold for judging if a voxel belongs to the bone. Assume D is the covariance matrix of the vector set. $\bar{A}_3(x, I)$ and $\bar{A}_4(x, I)$ are defined as

$$\bar{A}_3(x, I) = E(D) \text{ and } \bar{A}_4(x, I) = \sqrt{e(D)} / 2R. \quad (4)$$

Here, $E(\cdot)$ denotes the eigenvector corresponding to the largest eigenvalue $e(\cdot)$.

The four sub-vectors of $\bar{A}(x, I)$ jointly describes the distribution characters of bone density around each voxel. In Fig.1, we schematically demonstrate their geometric meanings. The gray and white regions represent the bone region and the background, respectively. The cross indicates the position of the voxel x under consideration. Solid circle denotes a spherical neighborhood of x . $\bar{A}_1(x)$ is the ratio of the gray region inside the x 's spherical neighborhood. The solid point is the mass center of the gray region inside the x 's spherical neighborhood, $\bar{A}_2(x)$. $\bar{A}_3(x)$ is represented by the dashed arrow. It denotes the largest variation direction of the bone tissue distribution. The length of the dash arrow measures the value of the largest variation, which is $\bar{A}_4(x)$.

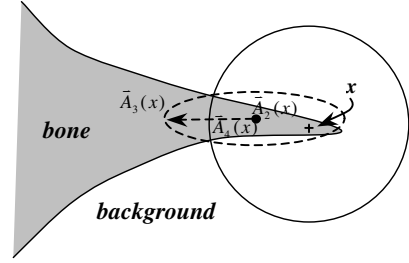


Fig.1 Schematic explanation on the geometric meanings of the attribute vector.

With the definition of attribute vector for each voxel in the images, the similarity of two voxels can be defined as the similarity of their attribute vectors. As the attribute vector is made up of sub-vectors that are almost independent with each other, the total similarity may be defined by simply summing up the respective similarities of sub-vectors. However, since the first sub-vector, i.e., the ratio of the bone tissues in the neighborhood of each voxel $\bar{A}_1(x, I)$, is the most distinctive feature in the attribute vector, we instead select a non-linear similarity criterion, which is dominated by the similarity of the first sub-vectors in the two attribute vectors. Mathematically, the similarity between a voxel x in the model image I_M and a voxel y in the subject image I_S is defined as:

$$S(\bar{A}(x, I_M), \bar{A}(y, I_S)) = \begin{cases} \sum_{i=1}^3 w_i S_i(\bar{A}(x, I_M), \bar{A}(y, I_S)), & \text{if } |\bar{A}_1(x, I_M) - \bar{A}_1(y, I_S)| \leq t_1 \\ 0, & \text{otherwise} \end{cases} \quad (5)$$

where

$$S_1(\bar{A}(x, I_M), \bar{A}(y, I_S)) = 1 - |\bar{A}_1(x, I_M) - \bar{A}_1(y, I_S)|$$

$$S_2(\bar{A}(x, I_M), \bar{A}(y, I_S)) = 1 - \|\bar{A}_2(x, I_M) - \bar{A}_2(y, I_S)\| / 2$$

$$S_3(\bar{A}(x, I_M), \bar{A}(y, I_S)) = e^{-\frac{(\bar{A}_3(x, I_M) - \bar{A}_3(y, I_S))^2}{2}} [(\bar{A}_3(x, I_M) \bullet \bar{A}_3(y, I_S) + 1) / 2]$$

and w_1, w_2, w_3 are parameters for adjusting the proportion of different parts in the total similarity function.

The ability of the attribute vectors in differentiating different parts of anatomical structures has been demonstrated in Fig. 2. We selected a voxel that is pointed by the yellow arrow as a reference point, and then calculated the similarities between the attribute vector of this reference point and the attribute vectors of all other voxels in the image. It can be observed from the color-

coded similarity map that only the voxels near the reference point have high similarities. That means, our attribute vector captures sufficient information to differentiate different anatomical structures of CT pelvis.

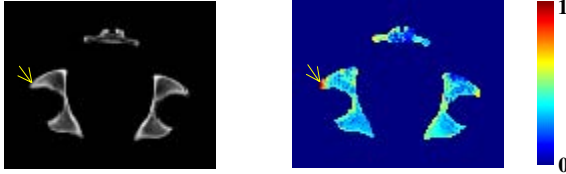


Fig.2 Demonstration of the ability of the attribute vector in differentiating the anatomical structures.

2.2. Energy function

Having defined the similarity between the attribute vectors of two voxels, we are ready to propose an energy function for evaluating the similarity between the transformed model and the subject images. Assuming V_M and V_S are the volumetric spaces of the model I_M and the subject I_S , respectively. x is a voxel in V_M . The transformation from the model to the subject is represented as $T(x) = x + \vec{d}(x)$, where $\vec{d}(x)$ is a displacement field; and the inverse transformation is $T^{-1}(x)$. The energy function is defined as following:

$$E = - \sum_{x \in V_M} [w_M(x) \sum_{z \in N(x)} S(\vec{A}(z, I_M), \vec{A}(T(z), I_S))] - \sum_{y \in V_S} [w_S(y) \sum_{z \in N(y)} S(\vec{A}(T^{-1}(z), I_M), \vec{A}(z, I_S))] + \sum_{x \in V_M} \|\nabla^2 \vec{d}(x)\| \quad (6)$$

The energy function has three characters that facilitate the robust computation of the optimal transformation.

First, the image similarity is not evaluated on individual voxels but on *subvolumes*, i.e., the spherical neighborhood of each voxel, $N(\cdot)$. In this way, the influence of individual voxel mismatching can be avoided.

Second, large weighting factors $w_M(x)$ are assigned to the voxels with the distinctive attribute vectors, since these voxels usually have fewer similar counterparts and thus are more reliable in finding their correspondences. In our case, as the attribute vector is more distinctive on the voxel that has larger boundary curvature, the weighting factor is designed to be proportional to the boundary curvature. (The method of calculating boundary curvature directly from grey image can be found in [14].) Weighting the energy term in this way allows the procedure to avoid the local minima in image registration.

Third, the energy function guarantees the consistency of transformations by jointly evaluating $T(x)$ and its inverse partner $T^{-1}(x)$. In Eq. 6, the first item of the energy function can be regarded as a force that pushes the voxel in the model space to the subject, while the second item can be regarded as a force that pulls the voxels in the model space from the subject. Such a design corresponds to the basic assumption for medical image registration, i.e., a diffeomorphic mapping [8] existing between the model and the subject images, and will lead to more consistent and biologically meaningful registration results.

The energy function is minimized by a set of hierarchical deformation strategies, as described in [8]. The resulting

transformation, $T_{opt}(x)$, describes the deformable transformation from the model to the subject.

3. RESULTS

To evaluate the performance of our method, we apply it on both synthesized and real CT images of male pelvises.

Synthesized images were created in the following way. First, we used the HAMMER algorithm [8] to elastically warp several real subjects to the space of the model. Then, we applied PCA on the obtained deformation fields, and collected the synthesized deformation fields by randomly sampling the subspace that was spanned by the principle components. Finally, the synthesized images were produced by warping the model image according to the synthesized deformation fields.

The performance of our registration method was demonstrated by comparing the differences of the algorithm-estimated deformation fields and the synthesized deformation field in two regions, i.e., the whole bone region and the pelvis boundary region. In the whole bone region, the average error and the max error are 1.28 mm and 4.32 mm, respectively, while in the boundary region, the average and the max errors are 0.67 and 1.29 mm, respectively. Shown as Fig.3, errors are relatively larger in the inner part of pelvis. This is because the voxels in those regions are very similar in both intensities and tissue distributions, which makes *definition* of proper point correspondence difficult. To further measure the registration errors, we evaluated boundary distance, overlap volume error and volume error between the model pelvis and registered synthesized pelvis. They are 0.5mm, 2.55% and 1.20%, respectively.

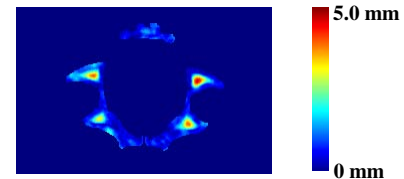


Fig.3 Color-coded errors between the synthesized deformation fields and the estimated deformation fields. The red denotes large error, while the blue denotes the small error. The range of errors is from 0 to 5.0 mm.

The performance of our method was also evaluated by five real male pelvises. The boundary distance, overlap volume error and volume error between the model pelvis and registered real pelvis are 0.64mm, 4.40% and 1.58%, respectively.

To visually check the accuracy of our registration method, we compared the average images generated by our method with the average image generated by affine registration method, on both synthesized and real images. As indicated in Fig. 4, our average images are sharper and clearer, which partially indicates the accuracy of our method in image registration.

The speed of our algorithm has been tested on a 500MHz processor of SGI workstation. The average running time for registering two images with the size of 256x256x150 is about 42 minutes.

4. CONCLUSION

In this paper, a method for pelvis registration has been proposed. After studying the characters of the pelvis CT images, a novel attribute vector was defined for each voxel, to reflect the density distribution of bone tissues around that voxel. By evaluating the similarity of attribute vectors in a non-linear way, different anatomical structures that look similar can be differentiated. Thus, the accurate registration of pelvis images was achieved by hierarchically establishing the correspondences between the image pairs during the procedure of deformable registration.

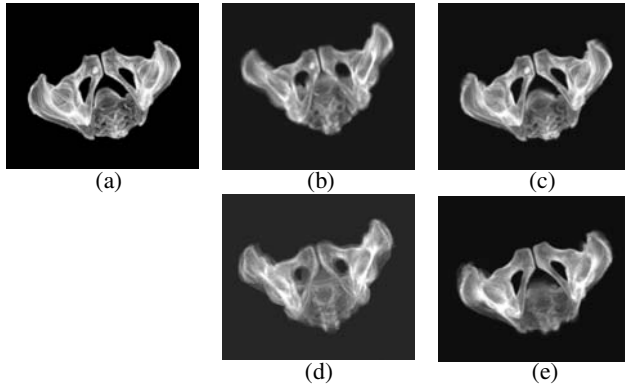


Fig.4 Visual comparison of affine registration method and our registration method in averaging the aligned pelvis CT images. 3D rendering images are displayed. (a) Model pelvis, (b) the average of 10 synthesized pelvises aligned by affine registration method, (c) the average of 10 synthesized pelvises aligned by our registration method, (d) the average of 5 real pelvises aligned by affine registration method, (e) the average of 5 real pelvises aligned by our registration method.

ACKNOWLEDGEMENT

Partial funding of this research was provided by the National Science Foundation under Engineering Research Center grant EEC9731748. We would also like to thank our colleagues Dr. Ted DeWeese, Anton Deguet, and Ofri Sadowsky of the Johns Hopkins University for their assistance in providing anonymous CT data and Dr. Christos Davatzikos of University of Pennsylvania for very helpful discussion.

REFERENCES

- [1] J.Yao, "A Statistical Bone Density Atlas and Deformable Medical Image Registration," *Ph.D Dissertation*, Johns Hopkins University, Dec. 2001
- [2] M. Holden, D.L.G. Hill, E.R.E. Denton, J.M. Jarosz, T.C.S. Cox, T. Rohlfing, J.Goodey and D.J. Hawkes, "Voxel Similarity Measures for 3D-Serial MR Brain Image Registration", *IEEE Trans. on Med. Imaging*, Vol. 19, pp. 94-102, 2000
- [3] U. Kjems, S. C. Strother, J. R. Anderson, and L. K. Hansen, "Enhancing the multivariate signal of [15O] water PET studies with a new nonlinear neuroanatomical registration algorithm", *IEEE Transaction on Medical Imaging*, Vol. 18: pp. 306-319
- [4] C. Davatzikos, "Spatial transformation and registration of brain images using elastically deformable models", *Computer Vision and Image Understanding*, Vol. 66, pp. 207-222, 1997
- [5] P. Thompson and A.W. Toga, "A surface-based technique for warping three-dimensional images of the brain", *IEEE Trans. on Med. Imaging*, Vol. 15, pp.402-417 1996
- [6] K.J.Friston, A.P. Holmes, K.J. Worsley, J.P.Poline, C.D. Frith and R.S.J. Frackowiak, "Statistical parametric maps in functional imaging: a general linear approach", *Human Brain Mapping*, pp. 189-210, 1995
- [7] G.E. Christensen, R.D. Rabbitt and M.I. Miller, "Deformable Templates Using Large Deformation Kinematics", *IEEE Trans. on Image Processing*, Vol.5, No. 9, 1996
- [8] D. Shen and C. Davatzikos, HAMMER: hierarchical attribute matching mechanism for elastic registration. *IEEE Transactions in Medical Imaging*, Vol 21, pp. 1421-1439, 2002
- [9] J.V. Hajnal, N. Saeed, E.J.Soar, A. Oatridge, I.R. Young and G.M. Bydder, "A registration and interpolation procedure for subvoxel matching of serially acquired MR images", *Journal of Computer Assisted Tomography*, Vol. 19, pp. 289-296, 1995
- [10] T.M. Buzug, J. Weese, C. Fassnacht and C. Lorenz, "Using an entropy similarity measure to enhance the quality of DSA images with an algorithm based on template matching", *Visualization in Biomedical Computing, Lecture Notes in Computer Science*, Berlin, Germany: Springer-Verlag, Vol. 1131, pp. 235-240, 1996
- [11] P.A. Viola, "Alignment by maximization of mutual information", Ph.D. thesis, Massachusetts Inst. Technology, Cambridge, MA, 1995
- [12] J.Weese, G.P. Penney, P.Desmedt, T.M. Buzug, D.L.G. Hill and D.J. Hawkes, "Voxel-based 2-D/3-D registration of fluoroscopy images and CT scans for image-guided surgery", *IEEE Trans. Inform. Technol. Biomed.*, Vol.1, pp.284-293, 1997
- [13] G.E. Christensen, "Consistent Linear-Elastic Transformations for Image Matching", *Information Processing in Medical Imaging*, LCNS 1613, Springer-Verlag, pp.224-237, 1999
- [14] O. Monga, R. Lengagne and R. Deriche, "Crest lines extraction in volume 3D medical images: a multi-scale approach", *Rapport de recherche 2338, INRIA*, 1994